

# Photoassisted Magnetization of Fullerene C<sub>60</sub> with Magnetic-Field Trapped Raman Scattering

Zhixun Luo,<sup>†</sup> Xiao Cheng,<sup>‡</sup> Yi Luo,<sup>‡</sup> Boon Hian Loo,<sup>§</sup> Aidong Peng,<sup>†</sup> and Jiannian Yao<sup>\*,†</sup>

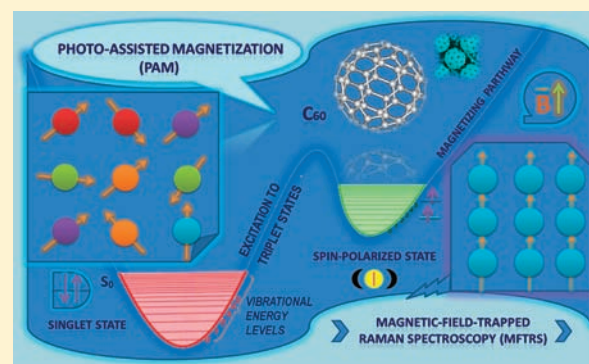
<sup>†</sup>Beijing National Laboratory for Molecular Science (Bnlms), and Key Laboratory of Photochemistry, Institute of Chemistry, The Chinese Academy of Sciences, Beijing, 100190, China

<sup>‡</sup>Theoretical Chemistry, Royal Institute of Technology, AlbaNova, S-106 91 Stockholm, Sweden and Hefei National Laboratory of Physical Sciences at the Microscale, University of Science and Technology of China, Hefei, Anhui 230026, P. R. China

<sup>§</sup>Department of Chemistry, Towson University, Towson, Maryland 21252, United States

**S** Supporting Information

**ABSTRACT:** We report a photoassisted method to magnetize microcrystal fullerene C<sub>60</sub> at room temperature by exciting it to triplet states via a proper laser radiation and then trapping the spin-polarized states under a strong magnetic field. Novel changes on Raman scattering of the C<sub>60</sub> microcrystals were observed in the presence and absence of the magnetic field. In particular, the Raman spectra were found to exhibit a “hysteresis” phenomenon when the external magnetic field was removed. In light of this, we propose magnetic-field-trapped Raman spectroscopy (MFTRS) and employ first-principle calculations to reproduce the Raman activities of C<sub>60</sub> at different states. Further, MFTRS of the fullerene is demonstrated to originate from its photoassisted magnetization (PAM). The PAM strategy enables the magnetization of materials which consist of only light elements; meanwhile, the MFTRS investigation may open a new research field in Raman spectroscopy.



## 1. INTRODUCTION

From the earliest description, known as lodestones around 2500 years ago, to the Tokamak equipment for nuclear fusion experiments nowadays, the explorations of magnets and magnetism accompany human history. It was previously concluded that ferromagnetism could not exist in the materials which consist only of light elements (e.g., carbon, hydrogen, oxygen, and nitrogen, etc.), where the interaction of unpaired electrons is negligible. However, in recent decades some carbon-based materials have been found to exhibit magnetic properties.<sup>1–10</sup> For example, pure graphite with topographic defects was found to give rise to local ferromagnetic states,<sup>2</sup> and weak spontaneous magnetization was also observed in heat-treated organic nitroxides;<sup>3</sup> in particular, an organic species C<sub>60</sub>-TDAE (tetrakisdimethylamino ethylene)<sup>11–13</sup> was extensively investigated with soft ferromagnetism at a Curie temperature of  $T_c = 16.1$  K. Besides, iodine-doped fullerene (I–C<sub>60</sub>) and cobaltocene-doped fullerene (Co–C<sub>60</sub>) were also found to bear irreversible magnetization in low temperature due to glass transition and spin of unpaired electrons of the fullerene cage.<sup>14,15</sup> Actually, the ring-current magnetic susceptibility of fullerene C<sub>60</sub> itself has been studied since its discovery in 1985.<sup>16–19</sup> However, it is still a challenge to establish the intrinsic properties in terms of the basic principles for traditional ferromagnets (based on 3d or 4f electrons).<sup>2,3</sup>

Along with these investigations which have speculated the existence of ferromagnetism in fullerenes and their derivatives,

the possibility to form a whole family of magnetic carbons with varying degrees of ferromagnetic content has been proposed at high temperature and with high-pressure treatments.<sup>20</sup> However, the exploration of new magnets for practical use may need to consider whether the materials are noncorrosive, biocompatible, and magnetically stable up to room temperature.<sup>6</sup> Thus, the approaches to magnetize fullerenes and carbon-based materials at room temperature become important. For this purpose, a better understanding of the correlations between the macroscopic properties (magnetism) and the microscale examination is a key to determine the related applications.<sup>21,22</sup>

Although the magnetic response of fullerenes could be different from planar aromatic hydrocarbons and graphite<sup>5</sup> which provide appropriate points of analogy for the  $\pi$ -electron energy structures,<sup>17</sup> there is a common basis for electron spins, spin polarization, and molecular states that are associated with the energy levels.<sup>13,18,23</sup> Herein, we report a magnetization strategy on microcrystal fullerene C<sub>60</sub> at room temperature by exciting it to triplet states via laser radiation and then trapping the spin-polarized states with a magnetic field. Raman spectroscopy is employed as the probe due to the fingerprint spectra regarding energy levels and molecular states,<sup>24,25</sup> and for the purpose of exciting C<sub>60</sub> to triplet states, a 514.5 nm Ar-

Received: September 27, 2011

Published: December 12, 2011

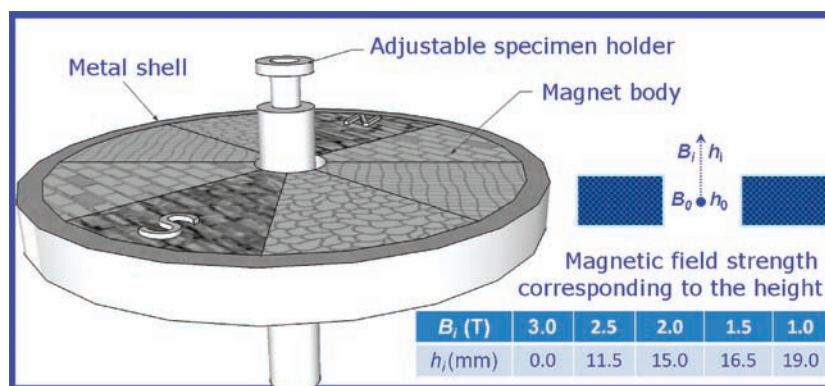


**Figure 1.** Sketch of the designed magnet. Special consideration of the size and magnetic-field strength was taken to fit the Raman spectrometer. An inset table shows the strength of the magnetic field corresponding to the distance from the hole-center of the magnet.

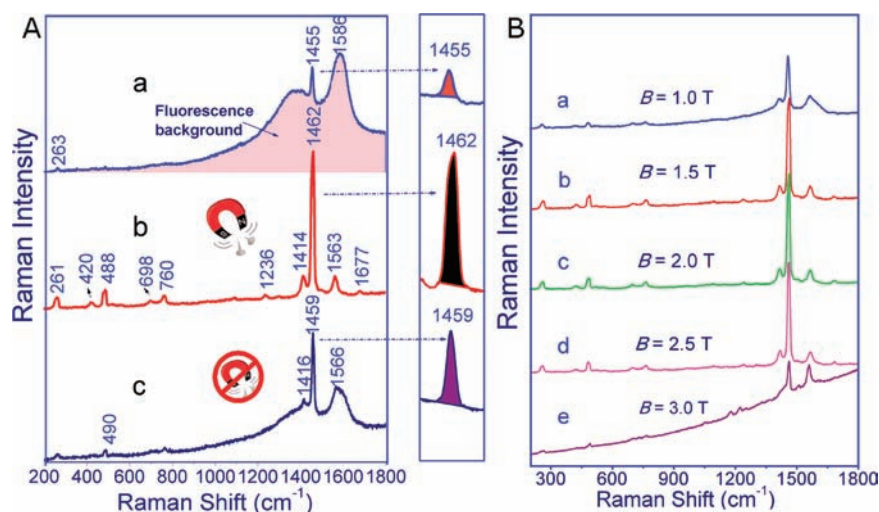


**Figure 2.** (A) 514.5 nm excited Raman spectra of solid  $C_{60}$  microcrystals in  $B = 0$  T (a), in  $B = 1.5$  T (b), and in  $B = 0$  T (c) taken 2 min after the removal of the applied magnetic field in (b). The inset figures on the right, respectively, show the magnified band at 1440–1480  $cm^{-1}$ . (B) Raman spectra of solid  $C_{60}$  microcrystals excited at 514.5 nm with different strength of the applied magnetic fields. (a)  $B = 1.0$  T; (b)  $B = 1.5$  T; (c)  $B = 2.0$  T; (d)  $B = 2.5$  T; and (e)  $B = 3.0$  T. These spectra were collected successively with the laser focused on the same spot and at the same power level.

ion laser was used in view of the lowest excited singlet state of the  $C_{60}$  (predominant  $T_{1g}$  and  $G_g$  characters)<sup>26</sup> and the resonance band at  $\sim 700$  nm.<sup>27</sup> As a result, magnetic-field-trapped Raman scattering (MFTRS) of the fullerene  $C_{60}$  was observed under the 514.5 nm excitation. Theoretical and experimental results provide vivid evidence for photoassisted magnetization (PAM) of the fullerene  $C_{60}$ .

## 2. EXPERIMENTAL SECTION

A specially designed magnet with appropriate dimensions to fit the Raman instruments was used, as shown in Figure 1. The magnet can be raised, lowered, and rotated without disturbing the inner sample lifting pillar. The magnetic field strength ( $B$ , corresponding to the distance  $h$  from the center of the hole) is listed in the table of Figure 1. The solid  $C_{60}$  samples (99.9% purity) consist of many microcrystals with sizes at several micrometers and a light absorption band at 250–700 nm (Supporting Information, Figures S1 and S2). The microcrystal samples, without further treatment, were filled in the sample socket of a lifting guide pillar which is movable to adjust the position of the sample.

The Raman spectra were collected on a Raman microprobe system (RENISHAW H1332S spectrophotometer) with the excitation line at 514.5 nm from an Ar ion laser and a line resolution of 4  $cm^{-1}$ . This Raman instrument employs a holographic notch filter and a charge-coupled device (CCD) to gain high detecting sensitivity. The Raman

band of a silicon wafer at 520  $cm^{-1}$  was used to calibrate the spectrometer before performing the experiments. The acquisition time was 10 s for each scan, with a total power at 15 mW (i.e., 3–5 mW on the sample surface). With the microprobe beam diameter of  $\sim 1$   $\mu m$ , the laser light could be readily focused onto a single microcrystal. Raman measurements were made at room temperature on many different microcrystals, with the long axis of the microcrystal parallel to the electric vector of the incident laser. The results were reproducible from microcrystal to microcrystal. For the experiments with applied magnetic fields, the direction of the field was made parallel to the electric vector of the laser excitation. In addition, a Bruker RFS 100/S FT-Raman spectrometer (1064 nm excitation) was also used, with a power at 50 mW and a line resolution of 3  $cm^{-1}$ .

## 3. RESULTS AND DISCUSSION

Figure 2A presents the 514.5 nm excited Raman spectra of  $C_{60}$  microcrystals (for details see Supporting Information, Figures S1 and S2) in the absence and presence of an externally applied magnetic field. The 514.5 nm Raman (without a magnetic field) of  $C_{60}$  in Figure 2A-a is distinguished by the prominent features in the 1400–1600  $cm^{-1}$  region, with two broad bands appearing at the  $\sim 1405$  and  $\sim 1586$   $cm^{-1}$  region, as well as a sharp peak of 1456  $cm^{-1}$  mode sandwiched between the two broad bands. In contrast to Figure 2A-a, however, the Raman spectrum in the presence of an applied magnetic field ( $B = 1.5$  T) shows well-

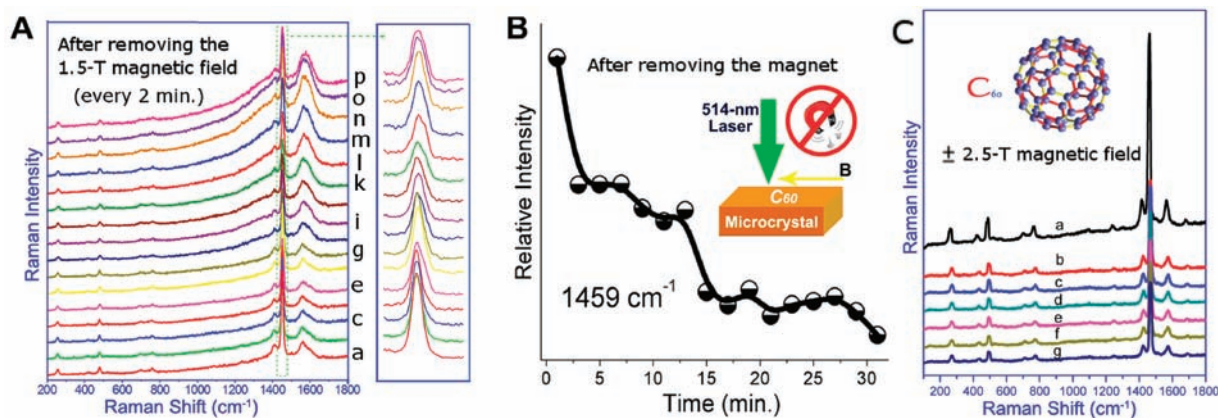


**Figure 3.** (A) Spectral features with time evolution measured after removing an applied magnetic field of 1.5 T. Each spectrum was excited at 514.5 nm and collected at 2 min intervals with the laser on continuously. (B) The relationship of the relative intensity of the  $1459\text{ cm}^{-1}$  mode as time changes on removal of the magnet. (C) Time-dependent Raman spectra of  $\text{C}_{60}$  excited at 514.5 nm with  $B = 2.5\text{ T}$  (a) and the spectra after removing the 2.5 T magnetic field (b ~ g), with each spectrum collected every 30 min with the laser off during each interval.

defined features, as given in Figure 2A-b. Besides the elimination of the fluorescence background, the differences between the two spectra (Figure 2A-a and 2A-b) involve the red/blue shifts (e.g., 263/261, 1455/1462, 1586/1563  $\text{cm}^{-1}$ ) and enhancements on the Raman intensities (e.g., an enhancement factor for  $I_{1642}/I_{1455}$  is found to be  $\sim 5$  via an evaluation based on integration area), and there is an additional peak appearing at  $1677\text{ cm}^{-1}$ . It is worth noting that Figure 2A-b also shows differences of peak values, half-widths (e.g., 261, 488  $\text{cm}^{-1}$ ), and relative intensities compared with a normal FT-Raman of the same solid  $\text{C}_{60}$  sample (Supporting Information, §2, Table S1 and Figure S3), as well as differences from the Raman of single-crystal  $\text{C}_{60}$ .<sup>28,29</sup> The distinguishing spectrum (Figure 2A-b) is named as MFTRS of the fullerene  $\text{C}_{60}$ .

Among the conditions to support a MFTRS observation of the fullerene  $\text{C}_{60}$  (e.g., a magnetic field at  $B \geq 1.0\text{ T}$ ), the best is attained when the field strength is  $\sim 2.5\text{ T}$ , as shown in Figure 2B. For the field strength at  $1.0\text{ T} < B < 2.5\text{ T}$ , the MFTRS spectra show almost the same spectral profile. However, at  $B = 3.0\text{ T}$ , the Raman spectrum differs from the others. As seen in Figure 2B-e, there is a monotonously increasing background, which indicates a “saturation effect” of MFTRS with the magnetic field strength. It is especially interesting to note that, after the magnetic field was removed, the spectrum (Figure 2A-c) did not fully revert to the initial spectrum before employing the magnetic field (Figure 2A-a). On the contrary, Figure 2A-c retained some of the same features as Figure 2A-b, which indicates a Raman spectral memory (“hysteresis”) for the fullerenes relative to the magnetic field. It happens that there is a similar case. Fullerene  $\text{C}_{70}$  was also found to exhibit similar MFTRS and “hysteresis” phenomena (for details see Supporting Information, Figure S7).

With an emphasis on the “memory effect”, we have measured time-dependent Raman spectra of the  $\text{C}_{60}$  for 30 min after removing the magnetic field. The results are shown in Figure 3A. Taking the  $1459\text{ cm}^{-1}$  mode as a representation, the variation of relative intensities over time is addressed in Figure 3B where a decay tendency can be observed (for more details see Supporting Information, Figure S4). Further, the “memory” ability was found to increase with the magnetic field strength and could last for a few hours (Figure 3C), while it was also found to weaken with doping of alumina (which was used as an

insulator for magnetic tunnel junctions<sup>30</sup>) (Supporting Information, Figures S5, S6).

These observations were primordially supposed to be attributed to magneto-optic effect, such as the Faraday effect, Cotton–Mouton effect,<sup>31</sup> Kerr effect,<sup>32</sup> and magnetization-induced second harmonic generation (MSHG),<sup>33</sup> etc. As is well-known, the Faraday effect is a result of ferromagnetic resonance which causes waves to be decomposed into two circularly polarized rays and leads to a rotation of the angle of linear polarization. Since the orientation of the magnetic field in this study has been designed to be vertical to the incident light instead of parallel to the direction of incident light, a possible influence from the Faraday effect is excluded. Besides, the Cotton effect refers to the double refraction of light in a liquid in the presence of a constant transverse magnetic field; the Kerr effect describes the changes of light reflected from magnetized media; and MSHG exists in some antiferromagnetic oxides (e.g.,  $\text{Cr}_2\text{O}_3$ ,  $\text{RMnO}_3$ ) and magnetic garnet films (e.g.,  $\text{CuB}_2\text{O}_4$ ,  $\text{CoO}$ , and  $\text{NiO}$ ).<sup>33</sup> In comparison with the nonapplicability of these effects, a Zeeman effect<sup>34,35</sup> could bring contributions via splits of spectral lines in the presence of a static magnetic field. However, analysis based on all of these magneto-optic effects cannot explain the excitation dependence, fluorescence quench, Raman enhancement, “saturation” effect, and “hysteresis” on MFTRS of the fullerenes. Furthermore, there is no MFTRS observation for carbon nanotubes (Supporting Information, Figure S8). Therefore, the MFTRS observation of  $\text{C}_{60}$  excludes a common origin based on the magneto-optic effect; instead, it probably results from a magnetization state of the fullerene which is different from its ground state and singlet excitation states.

In the ground state, the fullerene molecules in solid microcrystals follow a face-centered cubic stacking structure, where they keep a neighboring center-to-center distance at  $\sim 10\text{ \AA}$  and spin rapidly around their equilibrium lattice positions at room temperature. If an excitation (e.g., 1064 nm) is not enough to induce the  $\text{C}_{60}$  to excited states, the ground-state properties will be maintained. However, under a certain UV–vis excitation, fullerene  $\text{C}_{60}$  can transit from ground-state  $S_0$  to excited singlet states ( $S_1$ , or even  $S_n$ ), and then a finite population on the excited states transits to triplet states via a fast intersystem crossing.<sup>36–41</sup> It is important to note that there is only a small energy difference (i.e., 9 kcal/mol)<sup>41</sup> between

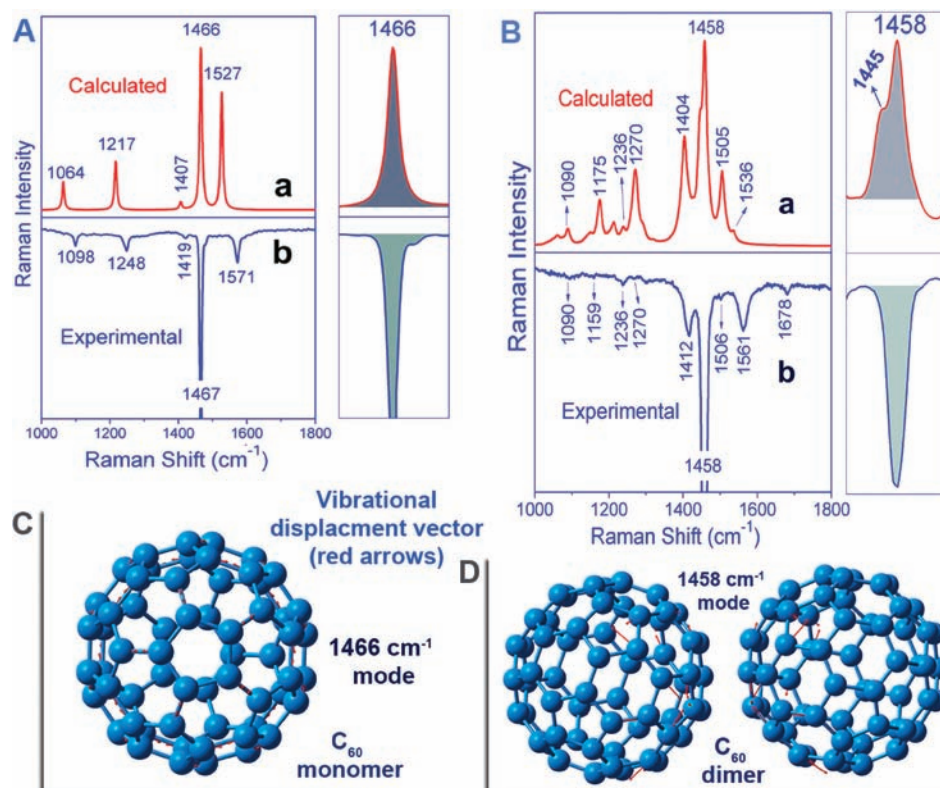


**Figure 4.** (A) Calculated Raman activity of a singlet-state  $C_{60}$  monomer (a), compared with a normal FT-Raman spectrum of solid  $C_{60}$  (b). (B) Calculated Raman spectrum of a quintet-state dimer  $C_{60}$  (a), compared with the 514.5 nm Raman of solid  $C_{60}$  in the presence of a  $B = 2.5$  T magnetic field (b). (C/D) The strongest vibrational modes of a singlet-state  $C_{60}$  monomer ( $1466\text{ cm}^{-1}$ ) and a quintet-state  $C_{60}$  dimer ( $1458\text{ cm}^{-1}$ ). The displacement vectors are shown with red arrows.

the first excited singlet state  $S_1$  and the triplet state  $T_1$ . Furthermore, the lifetime of the  $T_1$  state is much longer than that of the  $S_1$  states,<sup>36,40</sup> which ensures the triplet states of fullerene  $C_{60}$  are trapped by the external magnetic field and hence generate electronic spin polarization which results in local moments (of which the interaction can induce ferromagnetism in a large portion of the fullerene molecules).

We have employed the first-principle calculations (based on the Gaussian 03 software package)<sup>42</sup> to reproduce the Raman activities of fullerene  $C_{60}$  at different states (for details see Supporting Information, Figures S9–S13). First, the Raman activity of a single ground-state  $C_{60}$  molecule was calculated (Figure 4A-a), which accorded well with a FT-Raman spectrum excited at 1064 nm (Figure 4A-b). The accordance between them indicates that the vibrations of solid  $C_{60}$  at the ground state can be modeled by ignoring the crystal-field interaction and treating the  $C_{60}$  molecules as isolated singlet-state monomers. Second, we have also calculated the Raman activities of isolated triplet-state  $C_{60}$  monomers; however, the results differ much from all the experimental observations (Supporting Information, Figure S10). Finally, in view of the interaction of spin polarization, we have performed the modeling calculation with quintet states based on dimer  $C_{60}$  (Supporting Information, Figures S11, S12). As a result, the MFTRS of  $C_{60}$  (under a 514.5 nm excitation) is identified with the calculated Raman spectrum of a quintet-state  $C_{60}$  dimer at a gap distance of 2.20 Å (which is close enough to take into account the spin-polarized interaction, in comparison with 3.40 Å in usual states). Figure 4B shows the peak-to-peak accordance between the calculated and experimental spectra,

which confirms the proposal that the MFTRS originates from a different state of the fullerene  $C_{60}$ , generated by laser radiation and trapped by the magnetic field. It has been previously proved that the fullerene  $C_{60}$  molecules (in the excited states) can break through their equilibrium lattice positions and form polymerization under laser radiation.<sup>43,44</sup> The  $C_{60}$  in its crystalline form is held together by van der Waals forces which promise the conversion to the polymeric phase.<sup>6</sup> Together with electronic spin polarization and interaction in the magnetic field, polymerization of the  $C_{60}$  is associated with its magnetization,<sup>45</sup> with an energy difference at about 0.79 eV/ $C_{60}$  from our modeling calculations.

The polymerization of  $C_{60}$  molecules, followed by the magnetization, affects especially the frequency of the pentagonal pinch mode at  $1467\text{ cm}^{-1}$  in a normal Raman spectrum). This agrees with experimental observations and can be ascertained by comparing the vibrational displacement vectors of the most intense vibrational modes ( $1458\text{ cm}^{-1}$  band for a quintet-state  $C_{60}$  dimer and  $1466\text{ cm}^{-1}$  band for a singlet-state monomer), as shown in Figure 4C and D. The calculated Raman intensity for the  $1458\text{ cm}^{-1}$  mode is stronger ( $\sim 5.8$  times per  $C_{60}$ ) than that for the  $1466\text{ cm}^{-1}$  mode (Supporting Information, Figure S12), which is also coincident with the MFTRS results as mentioned above. On the other hand, the magnetization of  $C_{60}$  will also affect its fluorescence process since most of the  $C_{60}$  molecules stay in triplet states and quintet states (without a return to the ground state  $S_0$ ). This is also in accordance with the experimental observation (Figure 2A-b vs -a). It is worth mentioning that previous studies on theoretical calculations have predicted that electronic

instabilities in pure carbon can give rise to superconducting and ferromagnetic properties even at room temperature.<sup>10,21</sup>

On the contrary, the trapping process (of spin-polarized states) can also be released when removing the magnetic field, and thus the “polymerization” of  $C_{60}$  will separate again due to random thermal motion; subsequently, the decay allows a transition to the ground state ( $S_0$ ) via a gradual phosphorescence process.<sup>38,39</sup> When all the  $C_{60}$  molecules return to the ground state  $S_0$  with balanced lattice positions, they will recover the original properties, for instance, to conceive fluorescence again under an UV–vis excitation. The trapping and release of the spin-polarized states are identified with magnetization and hysteresis of the fullerene, as depicted in Figure 5.

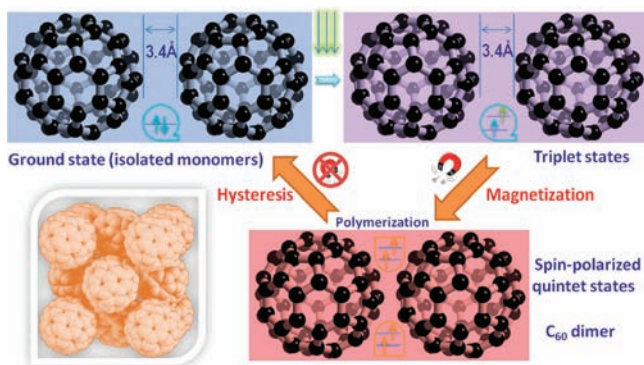


**Figure 5.** Sketch for the photoassisted magnetization and hysteresis process of fullerene  $C_{60}$ .

## CONCLUSIONS

We report a joint experimental and theoretical investigation on the nature of the fullerene  $C_{60}$  from a new perspective: magnetization at room temperature with photoexcitation assistance. Vivid evidence on the magnetization of  $C_{60}$  microcrystals is provided by observing the dramatic changes in Raman spectra (excited at 514 nm) in the presence and absence of a strong magnetic field. The photoassisted magnetization with verification of magnetic-field-trapped Raman scattering helps improve the understanding of the origins of magnetism in carbon-based materials and is applicable for magnetization of many other materials which consist only of light elements (C, H, O, N, etc.), even those with a filled electron shell where the total dipole moment is zero.

## ASSOCIATED CONTENT

### Supporting Information

Materials and methods, MFTRS demonstration, hysteresis, extending experiments, mechanism discussion, and more calculation details. This material is available free of charge via the Internet at <http://pubs.acs.org>.

## AUTHOR INFORMATION

### Corresponding Author

[jnyao@iccas.ac.cn](mailto:jnyao@iccas.ac.cn)

## ACKNOWLEDGMENTS

The authors thank Prof. Yan Fang (Capital Normal University), Prof. Tao Zhu (Peking University), Prof. Hongxing Xu (Institute of Physics, CAS), Prof. Zhongqun Tian (Xiamen

University), Prof. Wensheng Yang (Jilin University), and K. Don Dasitha Gunaratne (Pennsylvania State University) for their friendly discussions. Funding was provided by the National Natural Science Foundation of China (No. 20733006, 50720145202), the CAS/SAFEA International Partnership Program for Creative Research Teams, and the National Research Fund for Fundamental Key Project 973 (2006CB806200).

## REFERENCES

- Allemand, P.-M.; Khemani, K. C.; Koch, A.; Wudl, F.; Holczer, K.; Donovan, S.; Gruner, G.; Thompson, J. D. *Science* **1991**, *253*, 301.
- caronervenka, J. S.; Katsnelson, M. I.; Flipse, C. F. *Nature Phys.* **2009**, *5*, 840.
- Chiarelli, R.; Novak, M. A.; Rassat, A.; Tholence, J. L. *Nature* **1993**, *363*, 147.
- Esquinazi, P.; Setzer, A.; Höhne, R.; Semmelhack, C. *Phys. Rev. B* **2002**, *66*, 024429.
- Esquinazi, P.; Spemann, D.; Hohne, R.; Setzer, A.; Han, K.-H.; Butz, T. *Phys. Rev. Lett.* **2003**, *91*, 227201.
- Höhne, R.; Esquinazi, P. *Adv. Mater.* **2002**, *14*, 753.
- Mombrú, A. W.; Pardo, H.; Faccio, R.; Lima, O. F. d.; Leite, E. R.; Zanelatto, G.; Lanfredi, A. J. C.; Cardoso, C. A.; Araújo-Moreira, F. M. *Phys. Rev. B* **2005**, *71*, 100404 (R).
- Tanaka, K.; Yoshizawa, K.; Takata, A.; Yamabe, T.; Yamauchi, J. *J. Chem. Phys.* **1991**, *94*, 6868.
- Train, C.; Norel, L.; Baumgarten, M. *Coord. Chem. Rev.* **2009**, *253*, 2342.
- Makarova, T. L.; Sundqvist, B.; Höhne, R.; Esquinazi, P.; Kopelevich, Y.; Scharff, P.; Davydov, V. A.; Kashevarova, L. S.; Rakhmanina, A. V. *Nature* **2001**, *413*, 716.
- Kambe, T.; Kajiyoshi, K.; Fujiwara, M.; Oshima, K. *Phys. Rev. Lett.* **2007**, *99*, 177205.
- Mihailovic, D.; Arcon, D.; Venturini, P.; Blinc, R.; Omerzu, A.; Cevc, P. *Science* **1995**, *268*, 400.
- Narymbetov, B.; Omerzu, A.; Kabanov, V. V.; Tokumoto, M.; Kobayashi, H.; Mihailovic, D. *Nature* **2000**, *407*, 883.
- Mrzel, A.; Omerzu, A.; Umek, P.; Mihailovic, D.; Jaglicic, Z.; Trontelj, Z. *Chem. Phys. Lett.* **1998**, *298*, 329.
- Buntar, V.; Weber, H. W.; Ricco, M. *Solid State Commun.* **1995**, *98*, 175.
- Kroto, H. W.; Heath, J. R.; O'Brien, S. C.; Curl, R. F.; Smalley, R. E. *Nature* **1985**, *318*, 162.
- Elser, V.; Haddon, R. C. *Nature* **1987**, *325*, 792.
- Pasquarello, A.; Schluter, M.; Haddon, R. C. *Science* **1992**, *257*, 1660.
- Heiney, P. A.; Fischer, J. E.; McGhie, A. R.; Romanow, W. J.; Denenstien, A. M.; J., P. M. Jr.; Smith, A. B. *Phys. Rev. Lett.* **1991**, *66*, 2911.
- Wood, R. A.; Lewis, M. H.; Lees, M. R.; Bennington, S. M.; Cain, M. G.; Kitamura, N. *J. Phys.: Condens. Matter* **2002**, *14*, L385.
- Makarova, T. In *Studies of High-Tc Superconductivity*; Narlikar, A., Ed.; Nova Science Publishers, Inc.: New York, 2001; Vols. 44–45.
- Dresselhaus, M. S.; Dresselhaus, G.; Eklund, P. C. *Science of fullerenes and carbon nanotubes*; Academic: San Diego, 1996.
- Machtoub, L.; Tanaka, L.; Kito, H. *Physica C* **2006**, *445–448*, 478.
- Chen, M. S.; Shen, Z. X.; Liu, X. Y.; Wang, J. *J. Mater. Res.* **2000**, *15*, 483.
- Mishchenko, E. G. *Phys. Rev. B* **1996**, *53*, 2083.
- van den Heuvel, D. J.; van den Berg, G. J. B.; Groenen, E. J. J.; Schmidt, J.; Holleman, I.; Meijer, G. *J. Phys. Chem.* **1995**, *99*, 11644.
- Ikeda, K.; Uosaki, K. *J. Phys. Chem. A* **2008**, *112*, 790.
- Vibrational spectroscopy of  $C_{60}$* ; Menéndez, J., Page, J., Eds.; Springer: Berlin, 2000.
- Loosdrecht, P. H. M. v.; Bentum, P. J. M. v.; Verheijen, M. A.; Meijer, G. *Chem. Phys. Lett.* **1992**, *198*, 587.

- (30) Moodera, J. S.; Miao, G. X.; Santos, T. S. *Phys. Today* **2010**, April, 46.
- (31) Gifeisman, S. N.; Malkoch, Y. G. *Russ. Phys. J.* **1984**, 27, 355.
- (32) Weinberger, P. *Philos. Mag. Lett.* **2008**, 88, 897.
- (33) Fiebig, M.; Pavlov, V. V.; Pisarev, R. V. *J. Opt. Soc. Am. B, Opt. Phys.* **2005**, 22, 96.
- (34) Zeeman, P. *Nature* **1897**, 55, 347.
- (35) Pawlikowski, M.; Pilch, M.; Keiderling, T. A. *Chem. Phys.* **1993**, 178, 341.
- (36) Ebbesen, T. W.; Tanigaki, K.; Kuroshima, S. *Chem. Phys. Lett.* **1991**, 181, 501.
- (37) Groenen, E. J. J.; Poluektov, O. G.; Matsushita, M.; Schmidt, J.; van der Waals, J. H.; Meijer, G. *Chem. Phys. Lett.* **1992**, 197, 314.
- (38) Hung, W. C.; Ho, C. D.; Liu, C. P.; Lee, Y. P. *J. Phys. Chem.* **1996**, 100, 3927.
- (39) Sassara, A.; Zerza, G.; Chergui, M. *Chem. Phys. Lett.* **1996**, 261, 213.
- (40) Stepanov, A. G.; Portella-Oberli, M. T.; Sassara, A.; Chergui, M. *Chem. Phys. Lett.* **2002**, 358, 516.
- (41) Wasielewski, M. R.; Oneil, M. P.; Lykke, K. R.; Pellin, J. M. J.; Gruen, D. M. *J. Am. Chem. Soc.* **1991**, 113, 2774.
- (42) Frisch, M. J., et al. *Gaussian 03*, Revision B.05; Gaussian Inc.: Pittsburgh, PA, 2003.
- (43) Mathew, S.; Satpati, B.; Joseph, B.; Dev, B. N.; Nirmala, R.; Malik, S. K.; Kesavamoorthy, R. *Phys. Rev. B* **2007**, 75, 075426.
- (44) Rao, A. M.; Zhou, P.; Wang, K. A.; Eklund, P. C. *Science* **1993**, 259, 952.
- (45) Chan, J. A.; Montanari, B.; Gale, J. D.; Bennington, S. M.; Taylor, J. W.; Harrison, N. M. *Phys. Rev. B* **2004**, 70, 041403.